

## Experimental and Theoretical Studies for Corrosion Inhibition of Copper by 2,5-bis (ethyldisulfanyl)-1,3,4-thiadiazole in Rolling Oil

Sang Xiong, Jianlin Sun\*, Xudong Yan

School of Materials Science and Engineering, University of Science and Technology Beijing, Beijing 100083, China

\*E-mail: [sjl@ustb.edu.cn](mailto:sjl@ustb.edu.cn)

*Received:* 20 January 2016 / *Accepted:* 3 March 2016 / *Published:* 10 November 2016

---

The effect of 2,5-bis (ethyldisulfanyl)-1,3,4-thiadiazole (DTA) on the corrosion of copper in rolling oil containing aggressive additives was investigated by polarization, electrochemical impedance spectroscopy and weight loss measurement. The inhibition efficiency increases with the increase in concentration of inhibitors and temperature, below 373K. DTA acted as a kind of mixed-type inhibitor, the adsorption of inhibitors on copper surface obeys Langmuir isotherm and chemisorption mechanism. Kinetic model indicating the adsorbed DTA molecules on copper surface block the most active sites. Thermodynamics and quantum chemical calculations demonstrate that the adsorption configuration is found to be stable after corrosion inhibitor by itself decomposes, the sulfur-sulfur bonds are break and electrons are transferred from sulfur to carbon.

---

**Keywords:** Copper, Corrosion, Electrochemical impedance, Raman spectroscopy, Modelling

### 1. INTRODUCTION

Rolling oil is used extensively in several metal-processing industries and its residual onto copper surface is easy to oxidize [1; 2]. Using a suitable inhibitor in rolling oil is one of the effective methods for preventing corrosion [2]. Corrosion protection of organic inhibitors primarily by surface adsorption, which relies on the nature of metal surface in rolling oil and the structure features of inhibitor molecules [3; 4].

It is known that organic compounds with some electronegative functional groups and some conjugated heterocycle, indicating an inhibitory effect to corrosion of metal in acidic solutions [5]. Some compounds containing-nitrogen or sulfur functional groups and aromatic rings as inhibitors have

been reported in various media [4]. Heterocyclic thiadiazoles have been displayed excellent inhibition ability among these organic compounds. Yadav [6; 7] has been investigated 2,5-dimercapto-1,3,4-thiadiazole (DMTD) as corrosion inhibitor for copper in 3.5% NaCl solution by electrochemical technique and weight loss method. Heterocyclic DMTD contains N, S and thiadiazole ring that act as active sites during the adsorption [7]. Recently, some researches have been studied the inhibition of the corrosion of copper in 1.0 M H<sub>2</sub>SO<sub>4</sub> solution with and without DMDT, and it is found that three S atoms of DMTD adsorbs on copper surface to cause the high inhibition efficiency [8]. However, an investigation on the inhibition effect and mechanism of adsorption of DMDT derivate named 2,5-bis (ethyldisulfanyl)-1,3,4-thiadiazole (DTA) on the corrosion of copper in rolling oil has not been reported. The present work is to study the inhibition efficiency and the adsorption mechanism of DTA on copper in rolling oil. Weight loss and potentiodynamic polarization approaches were used to assess corrosion rate of copper samples and the inhibition efficiency of DTA. The surface morphologies were observed by scanning electron microscopy (SEM) and surface analysis was examined by surface enhanced Raman scattering spectroscopy (SERS). Moreover, the structural properties of DTA were obtained by quantum chemical method and the inhibition mechanism was studied based on molecular dynamic. We find that DTA is a kind of mixed-type inhibitor, the adsorption of inhibitors on copper surface obeys Langmuir isotherm and physisorption and chemisorption mechanism. The adsorption configuration is found to be stable after corrosion inhibitor by itself decomposes, the sulfur-sulfur bonds are break and electrons are transferred from sulfur to carbon.

## 2. EXPERIMENTAL

### 2.1. Materials preparation

Copper samples containing (weight %) Pb (0.0003), Si (<0.0005), As (<0.0001), P (0.0013), Sb (<0.0002), Ag (<0.0003), Zn (<0.0002), Te (<0.0002), Sn (<0.0005), Cd (0.0002), Fe (0.0009), Ni (<0.0005), Bi (0.0002) and balance Cu were used for electrochemical and weight loss studies [2]. The thickness of copper is 0.18 cm. Before each experimental run, copper samples were mechanically polished to <0.5 μm surface finish using diamond suspensions, ultrasonically cleaned with ethanol for 1 min, rinsed with ultrapure acetone, and dried in nitrogen gas dried at room temperature before being immersed in the rolling oil [2]. The aggressive solution (rolling oil) was performed using 0.2 wt% (wt% by weight) extreme pressure additives (a dialkyl dithiophosphate ester and nitrogen-containing boric acid ester) and 10 wt% oiliness additives (dodecanol and butyl stearate) prepared in copper rolling base oil [2]. The concentration range of DTA (purity > 98%) used was from 0.1 to 5.0 mM. The samples are put in the aggressive solution about 1 min and then fetched out for the electrochemical measurements.

### 2.2. Electrochemical tests

All electrochemical tests were conducted with an Autolab PGSTAT302 potentiostat/galvanostat. A criteria three-electrode electrochemical/corrosion electrochemical cell was used in all

tests. And a platinum electrode as the counter electrode was used. The reference electrode was a saturated calomel electrode (SCE). The tests were performed in a 150 ml volume cell at 373K using a water bath with temperature control. Before the tests, the working electrode was immersed in the deionized water for 30 min until a steady open circuit potential was obtained. For potentiodynamic polarization experiments the potential was scanned from -1100 to 0 mV at 1 mV/s. The EIS experiments were performed in the frequency range of  $10^6$  to  $10^{-2}$  Hz at open circuit potential.

Values of the  $E_i\%$  were calculated from polarization tests as below:

$$E_i(\%) = \frac{I_{corr}^o - I_{corr}}{I_{corr}^o} \times 100 \quad (1)$$

where  $I_{corr}$  and  $I_{corr}^o$  are the corrosion current densities obtained by the intersection of extrapolated cathodic and anodic Tafel lines in inhibited and uninhibited solutions, respectively.

### 2.3. Weight loss measurements

Square copper coupons (length = 5 cm, width = 5 cm) were used in weight loss experiments. The pretreated and weighed ( $m_0$ ) samples were immersed in glass beakers containing the aggressive solutions. All measurements were made in 200 ml of rolling oil solutions without and with various concentrations of DTA for 4 h. Then, the specimens were withdrawn and washed with ethanol in ultrasonic bath for 5 min, dried for 20 min, and weighed again ( $m$ ) using an analytical electronic balance accurate to 0.1 mg. The measurements were repeated 3 times and the data averaged in order to ensure the reliability of the results.

The value of corrosion rate was calculated from the following equation [9]:

$$v = \frac{m_0 - m}{S \cdot t} \quad (2)$$

where  $m_0$  and  $m$  are the mass of the copper coupon before and after immersion, respectively.  $S$  is the total exposed area of the square copper coupon,  $t$  is the corrosion time, and  $v$  is the corrosion rate. Inhibition efficiency of DTA ( $E_w\%$ ) for copper corrosion was obtained as below [10]:

$$E_w\% = \frac{v_0 - v}{v_0} \times 100 \quad (3)$$

where  $v_0$  and  $v$  are the corrosion rates of the copper coupon in rolling oil without and with the addition of inhibitor, respectively.

### 2.4. Surface morphology measurements

Surface morphology of copper was observed using SEM. The freshly polished and dried copper sample was placed in the sample platform, and the untreated surface was scanned to assess the bare surface before contact with rolling oil [11]. Raman spectroscopic measurements were conducted by using a confocal microprobe Raman system [11]. A liquid nitrogen-cooled 1024 × 800 pixels charge-coupled device was used as a detector, and an exciting line of 632.8 nm was supplied by a He-Ne laser with power of ca. 5 mW and a spot of the diameter ca. 3 mm on the copper surface [11].

A 50× long-working-length objective was used for focusing the laser spot onto the electrode surface. The slit and pinhole were set at 100 and 1000  $\mu\text{m}$ , respectively [11]. Each spectrum was measured three times, and the acquisition time was 20 s. Calibration was done referring to the 519  $\text{cm}^{-1}$  line of silicon [11].

### 2.5. Quantum chemical calculation

As we know, the molecular structure of the inhibitor plays a vital role in determining its mode of adsorption on the corroded surface [4]. The geometries of DTA were optimized by the Gaussian 03 software package employing the B3LYP/6-31G(d,p) method [12]. Semi-empirical molecular orbital calculations were performed to calculate the highest occupied molecular orbital (HOMO) and lowest unoccupied molecular orbital (LUMO) levels of DTA at ground state.

## 3. RESULTS AND DISCUSSION

### 3.1. Potentiodynamic polarization

**Table 1.** Potentiodynamic polarization data for Cu in deionized water in the absence and presence of DTA.

$C_{\text{inh}}(\text{mM})$	$\beta_{\text{c}}(\text{mVdec}^{-1})$	$\beta_{\text{a}}(\text{mVdec}^{-1})$	$R_{\text{p}}(\Omega\text{cm}^2)$	$E_{\text{corr}}(\text{mV})$	$I_{\text{corr}}(\mu\text{A cm}^{-2})$	$E_{\text{i}}(\%)$
Blank	205	24	8.3	-432	22.3	-
0.1	301	28	22.6	-486	7.5	66.37
0.5	314	33	36.4	-491	5.5	75.34
1.0	326	38	45.5	-502	4.2	81.65
2.5	346	42	58.7	-533	2.8	87.44
5.0	358	51	86.8	-564	1.8	91.93

The potentiodynamic polarization curves for copper containing residual oil in deionized water with different concentrations of DTA after 4 h of immersion time are presented in Fig. 1. The relevant electrochemical kinetic parameters, such as corrosion inhibition efficiency ( $E_{\text{i}}\%$ ), corrosion current density ( $I_{\text{corr}}$ ), polarization resistance ( $R_{\text{p}}$ ) and corrosion potential ( $E_{\text{corr}}$ ) as function of DTA concentration are given in Table 1.

Fig. 1 shows that both cathodic and anodic current densities decrease with the increase of DTA concentration, which indicates that the cathodic and anodic reactions are suppressed through DTA adsorption on the copper surface containing residual oil in deionized water. It is shown from Table 1 with the increase in DTA concentration, the values of  $I_{\text{corr}}$  decreased and  $E_{\text{i}}\%$  achieves to the maximum value at 5.0 m M DTA. Furthermore, both corrosion potential and current shift towards negative direction with the increasing DTA concentration. Basis of these studies, DTA is regarded as a mixed-type inhibitor for copper containing residual oil in deionized water. In addition, Tafel slopes are also increases with an increase in DTA concentration, indicating the activation of hydrogen evolution

reaction has controlled, and the mechanism of hydrogen evolution process do not affected by the presences of DTA [13].

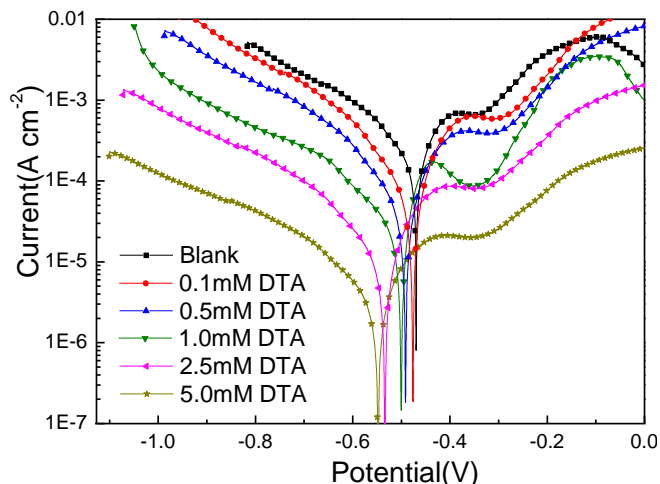


**Figure 1.** Potentiodynamic polarization curves for copper in deionized water without and with different concentrations of DTA (immersion 30 min, 373K, 1mV/s).

3.2. Electrochemical impedance spectroscopy

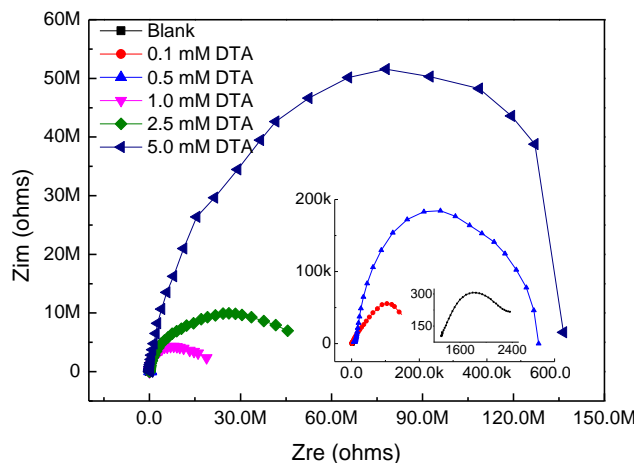


**Figure 2.** Nyquist plots for copper in deionized water containing different concentrations of DTA at 373 K.

Generally, kinetic information of electrode interface between the test solution and the copper can be given from the shape of the impedance diagram [14]. Fig. 2 shows the typical Nyquist plane plots of copper containing residual oil in deionized water in the absence and presence of various concentrations of DTA after immersion for 30 min at 373K. It is also found that the depressed semicircles are given at high frequencies, which relates to the loosening process of the electrical double-layer for the rapid charge transfer [15]. Afterwards, a number of irregular inductive loops are observed at low frequencies, which is associated with the loosening of the adsorbed intermediate process [15]. At the higher frequencies, those depressed cycle generally originated in the roughness

and other impurities of the copper surface [16], which is well-known “dispersion effect”. The diameters of capacitive loops also increase with the increasing DTA concentration, indicating the increase of charge transfer resistance and improving the inhibition effect of copper corrosion [17].

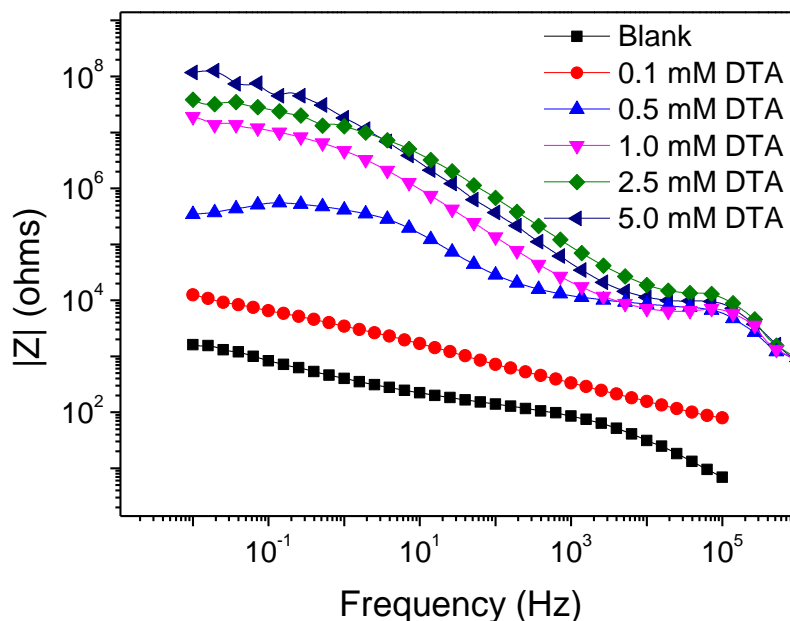


**Figure 3.** Bode plots for copper in deionized water without and with different concentrations of DTA.

The above impedance diagram observation can be verified by the Bode plots (Fig. 3). It reveals that the addition of DTA increases charge transfer impedance attributes to the protection film is formed on the copper surface. Considering that the value of charge transfer resistance is higher than that of diffuse resistance, the inhibition efficiency increased with the increasing inhibitor concentration, and it reaches a maximum value at 5.0 mM DTA. The inhibiting efficiencies obtained from EIS are in accord with the results got from the polarization measurements.

### 3.3. Weight loss studies

#### 3.3.1. Corrosion rate and inhibition efficiency

The corrosion rates of copper and the corresponding inhibition efficiencies in rolling oils containing various concentrations of DTA at different temperatures are shown in Fig. 4. It is clearly shown that the corrosion rates of copper reduce with an increase in DTA concentration and the temperature, below 373K. The corresponding inhibition efficiencies increase with the increasing DTA concentration till it achieves a maximum value at 373K. Above behavior attribute to the adsorption amount of inhibitor and the surface coverage on copper increase of the increasing DTA concentration, meanwhile desorption of DTA occurs at higher temperature [16].

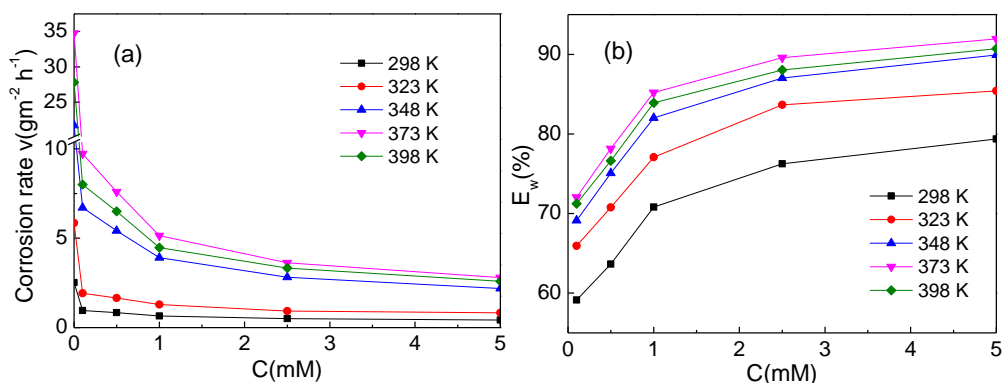


**Figure 4.** A plot of (a) corrosion rate (CR) and (b) inhibition efficiency (IE %) versus different concentration of DTA in rolling oil at different temperatures.

### 3.3.2. Adsorption considerations

Organic molecules adsorbed on the metal/solution interface to inhibit the corrosion and the interaction between metal surface and the inhibitor can be obtained from the adsorption isotherm [18]. Surface coverage ( $\theta$ ) is used to characterize inhibitor adsorption and the values of  $\theta$  were also calculated from weight loss experiment using the Sekine and Hirakawa’s method [18]:

$$\theta = \frac{v_o - v}{v - v_m} \times 100 \tag{4}$$

where  $v_m$  is the smallest corrosion rate at same temperature. All values of  $\theta$  are listed in Table 2.

**Table 2.** Surface coverage values obtained from the weight loss with various concentrations of DTA in rolling oil at different temperatures.

$C_{inh}$ (mM)	Coverage( $\theta$ )				
	298K	323K	348K	373K	398K
0.1	0.76	0.79	0.77	0.78	0.79
0.5	0.81	0.84	0.84	0.85	0.85
1.0	0.90	0.91	0.91	0.93	0.93
2.5	0.96	0.98	0.97	0.97	0.97
5.0	1.00	1.00	1.00	1.00	1.00

These  $\theta$  values were made to fit to a variety of isotherms, which was found the best fit for the Langmuir adsorption isotherm equation (Fig. 5):

$$\frac{C_{inh}}{\theta} = \frac{1}{K_{ads}} + C_{inh} \tag{5}$$

where  $C_{inh}$  is the concentration of inhibitor,  $K_{ads}$  is the adsorptive equilibrium constant, and  $\theta$  is the surface coverage. The obtained parameters, such as  $K_{ads}$ , linear regression coefficient ( $r$ ), and the maximum inhibition efficiency ( $E_w$ ) are placed in Table 3.

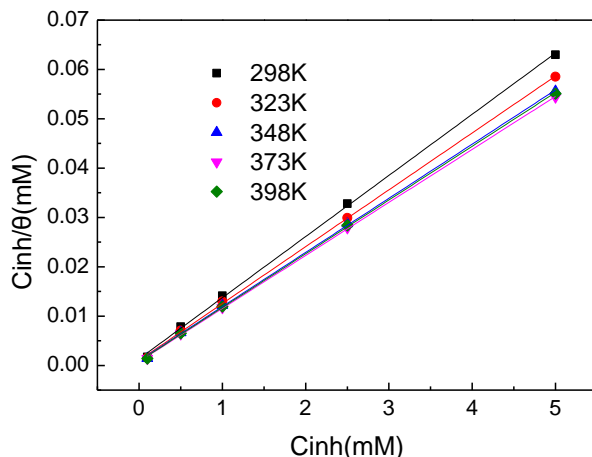


**Figure 5.** Curve fitting of the corrosion data for copper according to Langmuir thermodynamic kinetic model

**Table 3.** Linear regression parameters of the relationship of  $C_{inh}$  to  $C_{inh}/\theta$  for Cu in rolling oil at different temperatures.

Temperature(K)	$r$	Slope	Intercept	$K_{ads}$	Maximum $E_w$ (%)
298K	0.99996	0.9883	0.0729	137174.2	88.08
323K	0.99986	0.9861	0.0798	125313.3	88.14
348K	0.99983	0.9873	0.0844	118483.4	90.52
373K	0.99979	0.9885	0.0983	101729.4	92.33
398K	0.99987	0.9886	0.0757	132100.4	91.17

From Table 3, all the  $r$  and slopes are close to 1 and it is further to verify that the adsorption of DTA in rolling oil follows the Langmuir adsorption isotherm. In general,  $K_{ads}$  represents the interaction between adsorbent and adsorbate. The value of  $K_{ads}$  decreased with the increase in temperature before 373K and then increased after 373K, indicating that most efficient adsorption was obtained at 373K. So the highest inhibition efficiency is reach 92.33 % via adsorption of DTA on the copper surface.

The values of the standard free energy of adsorption were obtained as follow [18]:

$$\Delta G_{ads}^o = -RT \ln(55.5 K_{ads}) \tag{6}$$

where  $R$  is the gas constant and  $T$  is the absolute temperature and the value of 55.5 is the molar concentration of water in solution expressed in  $M^{-1}$ . According to the Van't Hoff equation [18]:

$$\ln K_{ads} = \frac{\Delta H_{ads}^o}{RT} + C \tag{7}$$

Thus, the adsorption enthalpy  $\Delta H_{ads}^o$  was got from the linear regression between  $\ln K_{ads}$  and  $1/T$  (Fig. 6). In the range of experimental temperature, the values of adsorption entropy and adsorption enthalpy can be considered as the standard adsorption entropy and adsorption enthalpy during the inhibition process.

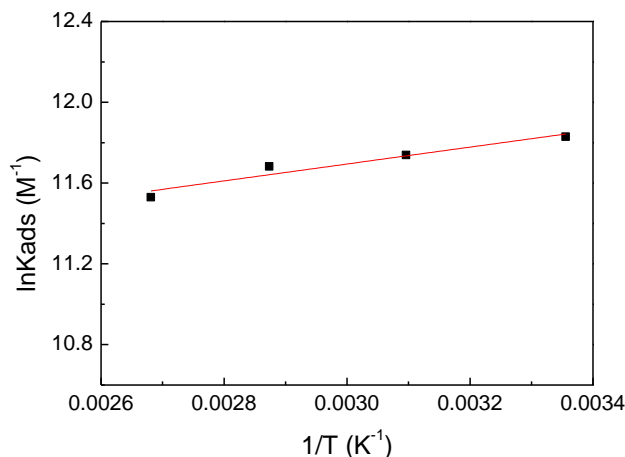


**Figure 6.** Van't Hoff plot for the Cu/DTA/rolling oil system.

Likewise, the standard adsorption entropy  $\Delta S_{ads}^o$  could be calculated from the thermodynamic basic equation:

$$\Delta G_{ads}^o = \Delta H_{ads}^o - T\Delta S_{ads}^o \quad (8)$$

All the calculated thermodynamic parameters are given in Table 4. The values of  $\Delta H_{ads}^o$  and  $\Delta S_{ads}^o$  indicate the adsorption of inhibitor is a spontaneous exothermic process. The inhibitor gradually replaced other molecules onto the copper surface; the replacement adsorption process can be a spontaneous exothermic and also relates to the increase in entropy of the solute, and the increase in entropy to be the driving force during the adsorption [19].

**Table 4.** Thermodynamic parameters of adsorption of DTA on the Cu surface at different temperatures.

Temperature(K)	$\Delta G_{ads}^o$ (kJ mol <sup>-1</sup> )	$\Delta H_{ads}^o$ (kJ mol <sup>-1</sup> )	$\Delta S_{ads}^o$ (kJ mol <sup>-1</sup> )
298	-39.26	153.74	647.64
323	-42.31	153.74	606.96
348	-45.42	153.74	572.30
373	-48.21	153.74	541.42
398	-52.31	153.74	517.71

The negative values of  $\Delta G_{ads}^o$  indicate the spontaneity of inhibitor molecule adsorption onto the copper surface. Values of  $\Delta G_{ads}^o$  up to  $-20$  kJ mol<sup>-1</sup> are always consistent with the electrostatic interaction between the charged molecules and the charged metal (physical adsorption), while those more negative than  $-40$  kJ mol<sup>-1</sup> involve charge sharing or transfer from the inhibitor molecules to the metal surface to form a coordinate type of bond (chemical adsorption)[20]. Actually, adsorption of organic molecules on metal surface is not only considered as a single physical or a single chemical adsorption process at 298K. The calculated values of  $\Delta G_{ads}^o$  are higher than  $-20$  kJ mol<sup>-1</sup> but less than  $-40$  kJ mol<sup>-1</sup>, which indicates that the adsorption of mechanism can be a chemical adsorption converted

from physical adsorption to or even a comprehensive adsorption at 298K. When the temperature is above 298K, DTA is adsorbed on copper surface forming chemical bond in the adsorption process.

### 3.3.3. Kinetic considerations

Kinetic model was conducted to further illustrate the inhibition properties of the inhibitor. The apparent activation energy for the corrosion process is calculated from the Arrhenius equation [20]:

$$\ln v = \frac{-E_a}{RT} + \ln A \tag{9}$$

where  $E_a$  represents the apparent activation energy,  $A$  is the preexponential factor, and  $v$  is the corrosion rate. The Arrhenius plots of  $\ln v$  versus  $1/T$  for the blank and various concentrations of DTA at different temperatures are given in Fig. 7. The values of  $E_a$  and  $A$  were calculated from the slopes and intercepts of the Arrhenius plots, respectively [20]. All the kinetic parameters are listed in Table 5. All the  $r$  is close to 1, suggesting that the copper corrosion in rolling oil can be explained using the kinetic model.

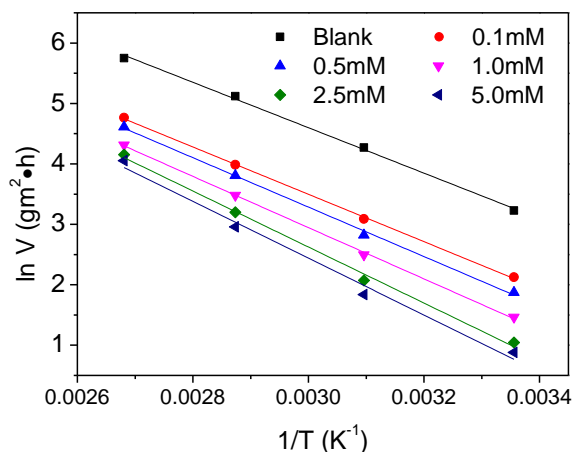


**Figure 7.** Arrhenius plots for copper in rolling oil without and with different concentrations of DTA.

**Table 5.** Kinetic parameters of the regression between  $\ln v$  and  $1/T$  for Cu in rolling oil containing different DTA concentrations.

$C_{inh}(mM)$	$E_a(KJmol^{-1})$	$A(gm^{-2}h^{-1})$	$r$
Blank	31.23	7.80E+12	0.99731
0.1	32.56	1.14E+13	0.99926
0.5	34.00	1.55E+13	0.99749
1.0	35.24	6.34E+12	0.99907
2.5	38.53	4.10E+13	0.9947
5.0	39.10	4.18E+13	0.9855

According to Eq. (9), the corrosion rate of copper relies on  $E_a$  and  $A$ . From Table 5, the value of  $A$  in the absence of DTA (Blank) is lower than that presence of DTA, so the higher corrosion rate of copper mostly depends on the lower apparent activation energy. The higher value of  $E_a$  was regarded

as physical adsorption that often occurred in the first stage [21]. Addition of inhibitor, the adsorption mode concerns the changes of the activation energy in corrosion process [22]. Assuming the electrochemical corrosion is heterogeneous reactions, the preexponential factor in the Arrhenius equation  $A$  is the number of active centers [23]. There are two possibilities about these active centers with different  $E_a$  on the metal surface: In the first case the activation energy in the presence of inhibitor molecules is higher than that of rolling oil ( $E_{a;inh} > E_{a;blank}$ ), the inhibitor is adsorbed on the most active adsorption sites (having the lowest energy) and the corrosion process occurs chiefly on the active sites (having higher energy). In the other case ( $E_{a;inh} < E_{a;blank}$ ), a smaller number of more active sites remain uncovered which take part in the corrosion process [10]. From Table 5, the values of  $E_a$  and  $A$  in the absence of inhibitor molecules are lower than that present of inhibitors in rolling oil, indicating that the adsorbed DTA molecules on copper surface inhibit the most active sites [22].

### 3.4. Surface morphology

Fig. 8 shows a SEM image of a fresh polished copper surface after corrosion test. When rolling oil is absence of inhibitor, there are irregular corrosion pits and the copper surface was strongly damaged with deep cavities. However, it is obvious that surface texture of rolled copper foil is clear with adding corrosion inhibitor and the result showed the inhibitors effectively prevent the surface corrosion. The protection of the copper surface is obtained by strong adsorption of the molecules and preventing it from being corroded easily [2].

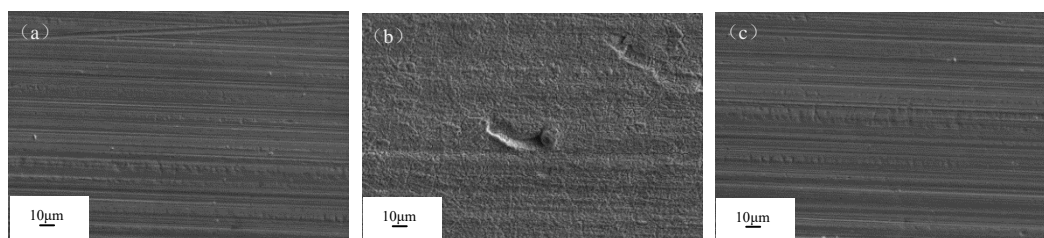


**Figure 8.** SEM image of (a) polished, (b) uninhibited and (c) inhibited copper samples surface

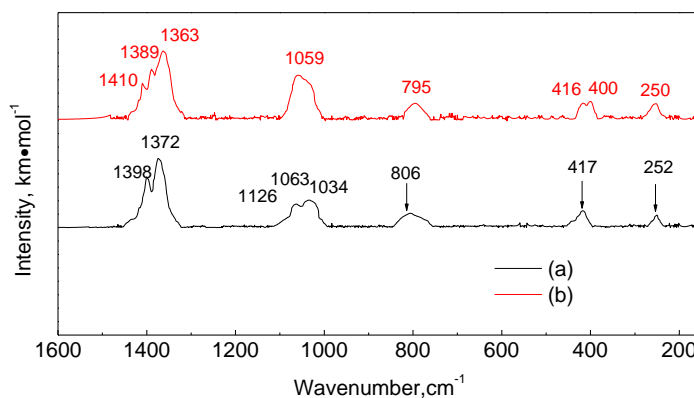


**Figure 9.** SERS spectra of (a) DTA powder and (b) the DTA film on the Cu surface

Monosulfide complex of thiadiazole derivate on copper surface by SERS spectra has been reported [11]. In order to obtain the surface character of copper immersed in rolling oil in the presence of DTA, the SRES analysis was studied. The SERS spectra of pure DTA powder and the adsorbed DTA film on the Cu surface are given in Fig. 9. There are similar SERS characteristic frequencies in both spectra. Adsorption peaks at  $1410\text{cm}^{-1}$ ,  $1389\text{cm}^{-1}$ ,  $1398\text{cm}^{-1}$ ,  $1372\text{cm}^{-1}$  and  $1363\text{cm}^{-1}$  arise from C = N stretching vibration in the ring. The weak band at  $1034\text{cm}^{-1}$  and  $1063\text{cm}^{-1}$  are attributed to N–N stretch vibration. The strong bands at  $1126\text{cm}^{-1}$  and  $1059\text{cm}^{-1}$  belong to C = S vibration. It is demonstrate that the DTA molecules are adsorbed on the copper surface by two N-atoms and several S-atoms, which is further elaborate in the next quantum theory calculations.

### 3.5. Quantum chemical calculations and inhibition mechanism

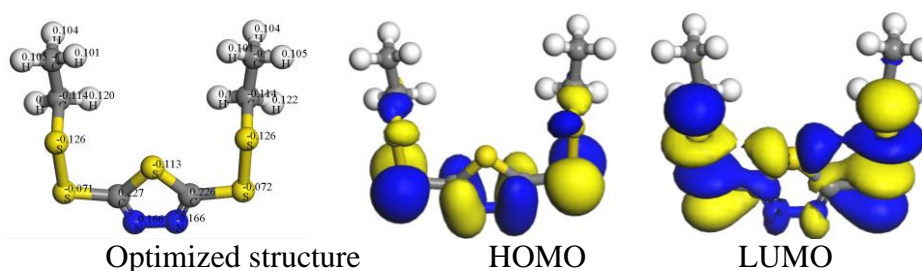
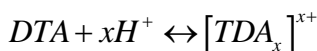


**Figure 10.** Optimized structure, server atom index, and HOMO and LUMO isosurfaces with a value of 0.017 a.u. for DTA molecule.

Mulliken charge distributions and server atom index of the optimized DTA molecule as well as the highest occupied molecular orbital (HOMO) and lowest unoccupied molecular orbital (LUMO) were calculated and shown in Fig. 10. It is given that the electron densities of both HOMO and LUMO are localized principally on two N atoms and five S atoms of thiadiazole rings, suggesting that these two N atoms and five S atoms are main active sites. The calculated quantum chemical parameters such as the energy of the highest occupied molecular orbital ( $E_{\text{HOMO}} = -5.599\text{ eV}$ ), energy of the lowest unoccupied molecular orbital ( $E_{\text{LUMO}} = -2.354\text{ eV}$ ), dipole moment ( $M = 2.756\text{ D}$ ), chemical potential ( $\mu = -3.976\text{ eV}$ ), chemical hardness ( $\eta = 1.62\text{ eV}$ ), global softness ( $S = 0.616\text{ eV}$ ), electrophilicity index ( $\omega = 9.745\text{ eV}$ ) and the energy gap,  $\Delta E$  ( $E_{\text{LUMO}} - E_{\text{HOMO}} = 3.245\text{ eV}$ ). The results demonstrate that DTA has the high value of chemical hardness and dipole moment, and low value of global softness and energy gap, which will conducive to enhancing inhibition by the adsorption of DTA on the copper surface.

Usually, there are two modes of adsorption as regards inhibitor adsorbed onto metal surface, the physical adsorption needs the presence of charged metal surface and charged species in the solution [24]. However, chemisorption process relies on the charge sharing or charge transfer from the inhibitor molecules to the metal surface [25]. Based on the obtained experimental and theoretical results, one possible inhibition mechanism of Cu in rolling oil could propose that DTA is a kind of mixed-type adsorption. In an aqueous solution, DTA molecule usually presences in the form of neutral molecules or cations because it is easy to protonated as follow [26]:



Then, the protonated DTA compete with the hydronium ions to minimize hydrogen evolution, which may be directly adsorbed at the cathodic sites to protect against copper corrosion and also plays an inhibition role in solutions [27]. Additionally, DTA molecules adsorbed on the electrode surface can be viewed as a process of DTA substitutes other molecules [28]. Further, since the surplus positive charge in corrosion potential of Cu surface, the negatively charged  $OH^-$  adhered to Cu surface by electrostatic attraction force [29]. So, the protonated inhibitor molecules can be attached on the copper surface with electrostatic interaction between inhibitor and  $OH^-$  cations. Generally, chemisorption is always accompanied with physical adsorption [30]. As more DTA adsorbed on the copper surface, electrostatic interaction also occurs through the  $\pi$ -electrons of thiadiazole ring transfer to the copper surface. At the same time, the DTA cations can accept electrons from the metallic surface in order to achieve electroneutrality and the feedback bond formed by overlapping  $3d$ -electrons from copper atom to the vacant  $3d$  orbital of S-atoms and N-atoms of thiadiazole rings [2]. From the point of view of thermodynamics, DTA adsorbed on a copper surface by itself decomposes (Fig. 11), the sulfur-sulfur bonds are break and electrons are transferred from sulfur to carbon, comprising a comprehensive physical adsorption and chemical adsorption, and it is further confirmed that the adsorption process includes not only the electrostatic interactions, but also electron donor-acceptor mutual effect [31].

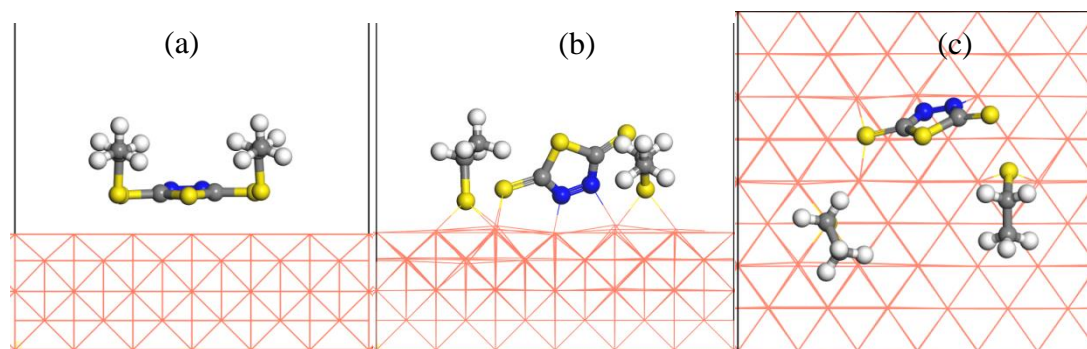


**Figure 11.** The most stable optimized structures of DTA chemisorbed on Cu surface: (a) side view of the initial configuration with DTA + Cu (110) slab; (b) side view of the optimization configuration with DTA + Cu (110) slab; (c) top view of the optimization configuration with DTA+ Cu (110) slab. Red lines are present copper atoms.

#### 4. CONCLUSIONS

(1) The DTA molecule is a kind of mixed-type inhibitor and mainly inhibits the cathodic corrosion of copper in rolling oil. The inhibition efficiency increases with the increase in concentration of inhibitors and temperature, below 373K

(2) The adsorption of DTA on the copper surface obeys the Langmuir adsorption isotherm and the values of  $\Delta G_{ads}^o$  and  $\Delta H_{ads}^o$  indicating the adsorption is a spontaneous exothermic and mixed adsorption process.

(3) SEM and SERS investigations also demonstrated that the adsorption of DTA on the copper surface can inhibit the copper corrosion in rolling oil.

(4) The experimental and theoretical results showed that DTA adsorbed on copper surface by itself decomposes, the sulfur-sulfur bonds are break and electrons are transferred from sulfur to carbon.

#### ACKNOWLEDGMENTS

The authors gratefully acknowledge the financial assistance provided by the National Natural Science foundation of China (No. 51474025).

#### References

1. C.G. Soares, Y. Garbatov, A. Zayed, and G. Wang, *Corros. Sci.*, 51 (2009) 2014-2026.
2. X. Sang, S. Jianlin, J. Wei, X. Yang, Z. Yingfeng, and X. Lei, *China Petroleum Processing and Petrochemical Technology*, 17 (2015) 96-107.
3. A. Döner, R. Solmaz, M. Özcan, and G. Kardaş, *Corros. Sci.*, 53 (2011) 2902-2913.
4. I. Jevremović, M. Singer, S. Nešić, and V. Mišković-Stanković, *Corros. Sci.*, 77 (2013) 265-272.
5. V. Pandarinathan, K. Lepková, S.I. Bailey, T. Becker, and R. Gubner, *Ind. Eng. Chem. Res.*, 53 (2014) 5858-5865.
6. M. Yadav, D. Behera, and S. Kumar, *Surf. Interface Anal.*, 46 (2014) 640-652.
7. M. Yadav, S. Kumar, and D. Behera, *Journal of Metallurgy*, 2013 (2013) 1-14.
8. W. Chen, H.Q. Luo, and N.B. Li, *Corros. Sci.*, 53 (2011) 3356-3365.
9. A. Marmur, *Langmuir*, 20 (2004) 1317-1320.
10. A.Y.I. Rubaye, H.T. Abdulsahib, and A.A. Abdulwahid, *Journal of Encapsulation and Adsorption Sciences*, 05 (2015) 155-164.
11. S. Xiong, J. Sun, X. Yan, Y. Xu, *Surf Interface Anal.* 48 (2016), 88-98.
12. H. Ju, Z. Kai, and Y. Li, *Corros. Sci.*, 50 (2008) 865-871.
13. W. Chen, H.Q. Luo, and N.B. Li, *Corros. Sci.*, 53 (2011) 3356-3365.
14. E. Brunk, and U. Rothlisberger, *Chem. Rev.*, 115 (2015) 6217-6263.
15. L. Feng, H. Yang, and F. Wang, *Electrochim. Acta*, 58 (2011) 4274-36.
16. W. Li, Q. He, C. Pei, and B. Hou, *Electrochim. Acta*, 52 (2007) 6386-6394.
17. E.M. Sherif, and S. Park, *Electrochim. Acta*, 51 (2006) 4665-4673.
18. S. Azizian, M. Haerifar, and J. Basiri-Parsa, *Chemosphere*, 68 (2007) 2040.
19. W. Chen, H.Q. Luo, and N.B. Li, *Corros. Sci.*, 53 (2011) 3356-3365.
20. M. Bouklah, B. Hammouti, M. Lagrenée, and F. Bentiss, *Corros. Sci.*, 48 (2006) 2831-2842.
21. H. Ashassi-Sorkhabi, B. Shaabani, and D. Seifzadeh, *Appl. Surf. Sci.*, 239 (2005) 154-164.
22. E.S.S.R. A. Popova, *Corros. Sci.*, 45 (2003) 33-58.
23. M.A. Amin, G.A.M. Mersal, and Q. Mohsen, *Arabian Journal of Chemistry*, 4 (2011) 223-229.A.
24. Popova, M. Christov, and A. Vasilev, *Corros. Sci.*, 49 (2007) 3276-3289.
25. M. Lebrini, M. Lagrenée, H. Vezin, L. Gengembre, and F. Bentiss, *Corros. Sci.*, 47 (2005) 485-506.
26. K.F. Khaled, and S.S. Abdel-Rehim, *Arabian Journal of Chemistry*, 4 (2011) 397-402.
27. H. Zarrok, A. Zarrouk, R. Salghi, H. Oudda, B. Hammouti, M. Ebn Touhami, M. Bouachrine, and O8H. Pucci, *Portugaliae Electrochimica Acta*, 30 (2012) 405-417.
28. B.H.S.S. A. Zarrouk, *Int. J. Electrochem. Sci.*, (2012) 5997-6011.
29. Y. Kayaba, H. Tanaka, and S.S. Ono, *The Journal of Physical Chemistry ,C* 119 (2015) 22882-22888.

30. R.T. Loto, C.A. Loto, A.P.I. Popoola, and T.I. Fedotova, *Portugaliae Electrochimica Acta*, 32 (2014) 337-354.
31. B.H.H.Z. A. Zarrouk, *Int. J. Electrochem. Sci.*, 6 (2011) 6261-6274.

© 2016 The Authors. Published by ESG ([www.electrochemsci.org](http://www.electrochemsci.org)). This article is an open access article distributed under the terms and conditions of the Creative Commons Attribution license (<http://creativecommons.org/licenses/by/4.0/>).